SCIENCE TARGET PRIORITIZATION FRAMEWORK FOR REMOTE SENSING

Vinay Ravindra[1,2], Douglas Caldwell[1,3], Meghan Chandarana Saephan[1], Bryan Duncan[4], Sarah Strode[4,5], William Swartz[6], Kristen Manies[7], Jeremy Frank[1], Richard Levinson[1,8], Eugene Turkov[1]

[1]NASA Ames Research Center, [2]Bay Area Environmental Research Institute, [3]SETI Institute, [4]NASA Goddard Space Flight Center, [5]Morgan State University, [6]Johns Hopkins University Applied Physics Laboratory, [7]U.S. Geological Survey, [8]KBR/Wyle

ABSTRACT

Behind the scenes of a remote sensing mission there are complex decision making and planning operations. Streamlining these operations, with a quantitative scientific value framework, aids efficient and optimized science data collection. While there have been previous efforts to quantify the science value for specific science scenarios, our work aims to develop a general framework which can be applied across different scenarios. We describe a pipeline of processes which combines model forecast and observation data, in computational forms, as dictated by the mission objectives set forth by subject matter experts. The framework is described with use cases involving the monitoring of nitrogen dioxide (NO2) concentrations over the Gulf of Mexico and methane concentrations over interior Alaska.

Index Terms— remote sensing, mission operations, forecast, planning, UAV

1. INTRODUCTION

Earth science sensors are flown on numerous platforms, such as aerial vehicles, balloons, and satellites. They are typically expensive as they acquire science-quality (i.e., well calibrated, stable) data, and, subsequently, a great deal of effort is involved in planning their deployment. In particular, field campaigns that involve aircraft platforms, including uncrewed aerial vehicles (UAVs), require rapid target selection based on environmental conditions. Traditionally, these targets are manually chosen by subject matter experts. This process is often tedious, slow, and relies on intuition acquired over years of experience. The Intelligent Long Endurance Observing System (ILEOS) project aims to develop a science planning framework that leverages science domain knowledge to fuse available data and identify high value science targets [1][2]. These targets can then be prioritized for observation.

There has been previous work in the context of assigning priority and science value for specific applications. For example, in [3] satellite observation locations were prioritized with data from flood-forecast model, in situ stream gauge and soil moisture sensors. Studies in [4][5][6] prioritized satellite synthetic aperture radar observations based on soil moisture uncertainty forecasts for effective global soil moisture monitoring. The study in [7] prioritized Global Navigation Satellite System-Reflectometry measurements over area of high wildfire danger. In [8], the authors combined historical snow water equivalent (SWE) data from the Copernicus ERA5-Land reanalysis dataset for an effective snow observations mission design problem. Our contribution is in the development of a generalized framework which could be customized to different science cases.

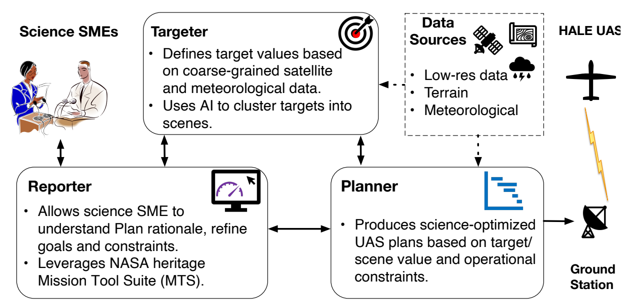

Figure 1: Role of Targeter during remote-sensing operations being developed for the Intelligent Long Endurance Observing System (ILEOS) project [1][2] which explores the planning of High Altitude Long Endurance (HALE) UAV flights for Earth science.

2. TARGETER OVERVIEW

Scheduling an observation consists of two primary components: (1) characterization/quantification of the science value (prioritization) of the observation, and (2) planning the platform(s)/instrument(s) operations. In this article we will focus on (1) which will be referred to as the Targeter. (2) will be referred to as the Planner. Figure 1 illustrates the entire ILEOS system framework. The scientists drive the system, with the Reporter as an interface to the Targeter and the Planner [1][2]. The primary characteristics to be considered in the Targeting framework are described below.

2.1 Science Objective

The end-users of the collected data are either scientists who focus on research and/or practitioners who apply the collected data for practical applications. For example, measuring

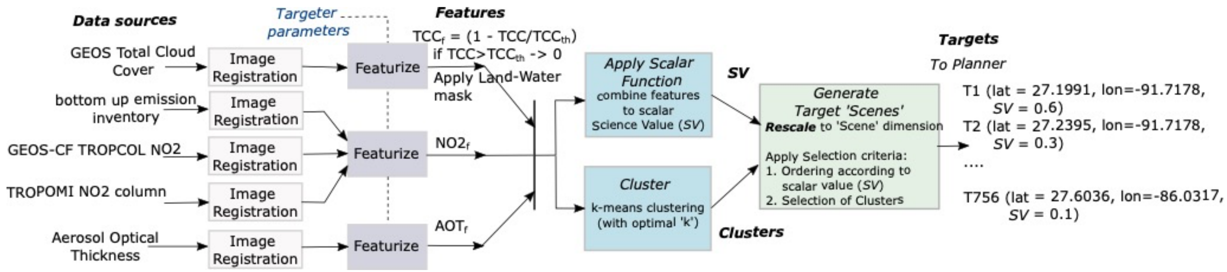

Figure 2: Targeter pipeline. The data-sources (left) are registered onto a common grid. 'Features' are built, and a scalar Science Value (*SV*) term is calculated. Areas with common characteristics are clustered. Finally, the *SV* is re-gridded to the resolution = scene dimension to give Targets. The Targets may be re-generated by tuning the Targeter parameters, until satisfaction.

pollutants would help scientists in the development of air quality models, and a practitioner in quantifying the emissions from known high-intensity sources (e.g., oil rigs). The science objective is provided by the scientists/ subject matter experts (SMEs) in a computational form which is based on numerical datasets (see below).

2.2 Numerical datasets

The basis of automated target prioritization is the use of *numerical* datasets, upon which the computational form of the use case objectives is evaluated. There are primarily two types of datasets which need to be considered:

Model-based: Science models, such as numerical weather prediction (NWP) models issue global/ regional forecasts of geophysical quantities (e.g., cloud cover, precipitation) in a comprehensive gridded format. These are essential to prioritize/de-prioritize targets across space & time.

Observed/Estimated: These could be satellite observations taken prior to the planned measurement campaign or data from emissions inventories or land-cover datasets.

2.3 Iterative feedback

Through the use of tunable values known as 'Targeter parameters', use case objective functions provide flexibility to the user to adjust the science values. The parameters are used to adjust the relative weights given to different inputs. Further, by the introduction of conditional statements, different computational forms itself can be chosen. This gives users the opportunity to tweak the parameters in real time and visualize the resulting prioritized targets through the Reporter interface.

3. TARGETER PIPELINE

The pipeline of processes within the Targeter (Figure 2) is described in this section with the aid of a science use-case concerning monitoring concentrations of nitrogen oxides (NOx: NO2, NO) over the Gulf of Mexico. A sample set of target locations/times was developed for a hypothetical flight campaign on 27th June 2023.

3.1 Science Objective

In this use case, users wanted to optimize data collection using High Altitude Long Endurance (HALE) UAVs equipped with an instrument capable of measuring NO2, to observe concentrations associated with oil and natural gas activities in the Gulf of Mexico. Their objective is to use the data to constrain emissions from these sources, which may be used as input to air quality models, for instance.

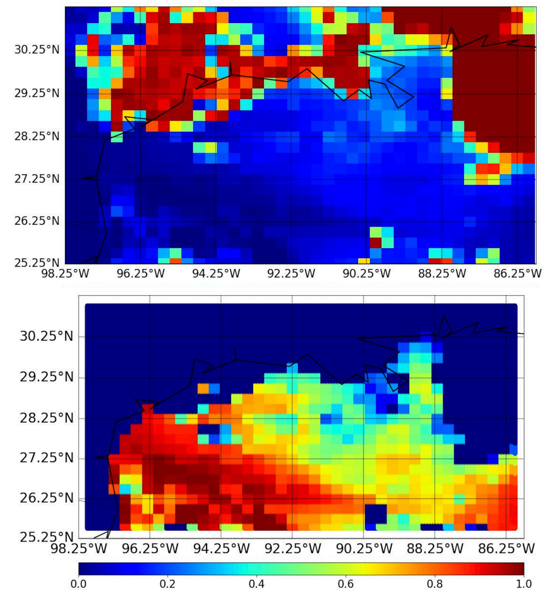

Figure 3: Gulf of Mexico NO2 case: Cloud-Total (top) from GEOS-FP. Cloud-feature (bottom). (Table 1 row1)

3.2. Registration onto common grid/scale

The underlying numerical data comes from a variety of sources and can potentially be at different coordinate frames, resolutions, and grids. All the data are re-gridded to a common grid by suitable interpolation schemes to ease application of mathematical operations. The grid resolution is chosen to match the finest resolution amongst the datasets. However, if the data handling times (file transfers, loading, etc.) become cumbersome, the resolution is made coarser, but is constrained to be less than the swath size of the instrument.

In the NO2 use case in the Gulf of Mexico, we used forecast data from chemical weather forecasts (GEOS-FP and GOES-CF [9]), satellite sensors (TROPOMI [10]), and a bottom-up emission inventory, which were all gridded within a rectangular domain in the Gulf of Mexico at 1.125 km resolution (<4.5km swath at 60k feet altitude for the NO2

Table 1: Features and data sources for the Gulf of Mexico NO2 use-case. A land-water mask based on GEOS-FP inst3_3d_chm_Np 'LWI' variable is applied to focus observations over water only. Targeter parameters are in bold-green. The values used for the test scenario is given in brackets.

Feature	Data source	Description
$f_{cld} = \max(0, 1 - cld/\boldsymbol{cld_{th}})$ cld is cloud cover cld_{th} is threshold value (0.3)	GEOS-FP tavg1_2d_rad_Nx; CLDTOT variable	Prioritize areas with better visibility for the instrument (Fig 3) > Less/no-cloud areas. > Areas with less aerosol Note the GEOS-FP forecasts are those issued 0 UTC cycle of the day (of action).
$f_{AOT} = \max(0, 1 - AOT/\boldsymbol{AOT_{th}})$ AOT is aerosol optical thickness AOT_{th} is threshold value (0.7)	GEOS-FP tavg3_2d_aer_Nx; TOTEXTTAU variable	
$f_{NO2} = \boldsymbol{w_P}\ \overline{PlatformEmis} + \boldsymbol{w_{NP}}\ \overline{NonPlatformEmis} + \boldsymbol{w_{Trp}}\ \overline{Tropomi_{NO2}}$ Weighted sum of the normalized emissions from inventory and satellite (Tropomi) observations. w_P, w_{NP}, w_{Trp} are user set weights. (1/3, 1/3, 1/3) nominally, and (1/2, 1/2, 0) when there is large continental influence over the Gulf of Mexico.	Bottom up emissions inventory, Vertical column NO2 data of Tropomi downscaled to 0.01km2. GEOS-CF xgc_tavg_1hr_g1440x721_x1; TROPCOL_NO2 as measure of NO2 from land.	Prioritization across platform, non-platform and Tropomi observations is adjusted using the weights. The weight to the satellite observation data can be set to '0' where/when the GEOS-CF forecast (12 UTC cycle of the previous day) is above a user-set threshold set by the parameter $\boldsymbol{ContInf_{th}}$ (4e15 molec cm-2).

Resulting Science Value in terms of the features is: $SV_{NO2} = f_{NO2}\ f_{AOT}\ f_{cld}$

sensor). TROPOMI tropospheric NO2 column densities [11] were re-gridded to 0.01°x 0.01° using the technique described by [12] and averaged over Mar 2018 through Apr 2022 by Daniel L. Goldberg (George Washington University, personal communication).

3.3. Feature Creation (from science objective)

The objective is given a mathematical representation in terms of "parameterized features", where each feature represents an aspect of interest. These features are combined to yield a 'Science Value (SV)' term. The features for the NO2 scenario are given are given in Table 1 and the $SV_{NO2} = f_{NO2}\ f_{AOT}\ f_{cld}$. The Targeter parameters are indicated in bold. Application of this equation to different forecast times results in a time-series of feature values over the course of a day (Fig 4), resulting in time-dependent priority which allows for collecting data at optimal times.

3.4. Clustering

Clustering can be applied on the vector of features to give quick snapshot to the users, of areas which have an overall common characteristic. It can also be used to provide *explainability* to the users on why certain areas are a priority.

We use k-means clustering, (**'k'** is the # clusters, and a Targeter parameter). Fig. 5 and Table 2c, which show the results of clustering (k=6) for the Gulf of Mexico NO2 case feature data at 15:30ET (27th June 2023). The table entries show the mean feature values of a particular cluster. Cluster #6 has the best visibility since it has the best cloud and AOT features. Cluster #4,5 have the best NO2 feature. From Table 2, we see that increasing k, results in decreased granularity. k=2 results in 2 areas where the decision on which area to observe is straightforward (i.e. cluster #2). k>2 results in clusters where there is potentially a tradeoff in the features.

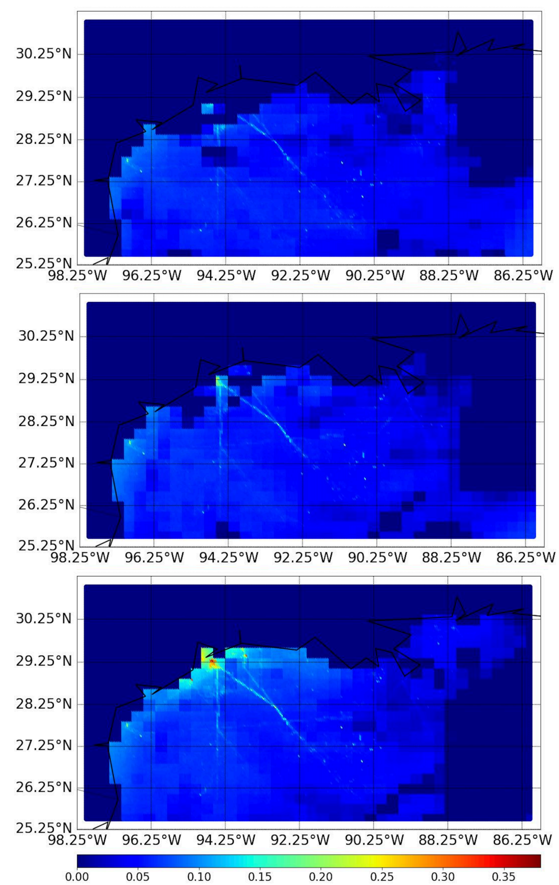

Figure 4: Gulf of Mexico NO2 Case: Temporal evolution of the Science Values (SV) of the Targets on 27 June 2023. (top->9:30ET, middle->12:30ET and bottom->15:30ET). High emission point-NO2 sources are not easily visible, unless zoomed.

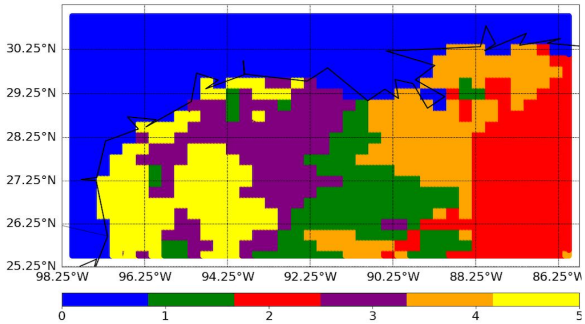

Figure 5: Gulf of Mexico NO2 case: Clusters formed (*k*=6) corresponding to the feature data of 15:30 ET, 27 June 2023. See mean cluster values in Table 2c.

Table 2: Mean cluster values for different *k* (Targeter parameter)

(a) *k* = 2

#	Cloud	NO2	AOT
1	0	0	0
2	0.54	0.10	0.78

(b) *k* = 4

#	Cloud	NO2	AOT
1	0	0	0
2	0.84	0.10	0.81
3	0.46	0.11	0.77
4	0.01	0.09	0.74

(c) *k* = 6

#	Cloud	NO2	AOT
1	0	0	0
2	0.62	0.09	0.81
3	0.01	0.09	0.74
4	0.80	0.11	0.80
5	0.38	0.11	0.76
6	0.96	0.10	0.81

3.5. Target Scene Generation

The gridded *SV* is re-gridded (with suitable interpolation) to the resolution equal to the scene size (= swath size, 4.5 km for the NO2 sensor). These values represent the priority of the location. The users may then choose to select a subset of the targets based on the clusters, depending on the use-case. For example, if a high SNR (good visibility) observation was desired irrespective of the NO2 feature, then cluster #6 (Table 2c) would be chosen.

3.6. Methane concentrations at Interior Alaska

Another case study focused on monitoring for methane concentrations from biogenic emissions in interior Alaska. The users were interested in discovering new methane sources by using satellite data and obtaining high resolution HALE based imagery using AVIRIS-NG instrument [13] over areas with landcover types that have high potential for methane emissions. Figure 6 shows the different features built based on cloud forecast, (sparse) GOSAT XCH4 Dry air mole fraction data [14,15,16], and landcover [17,18].

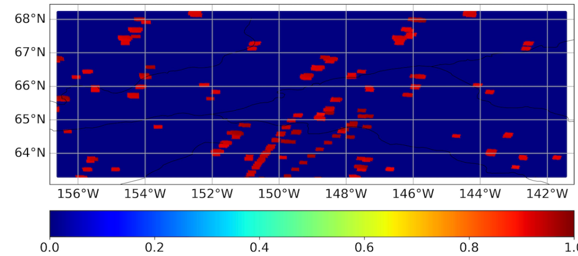

(a) GOSAT mean CH4 feature

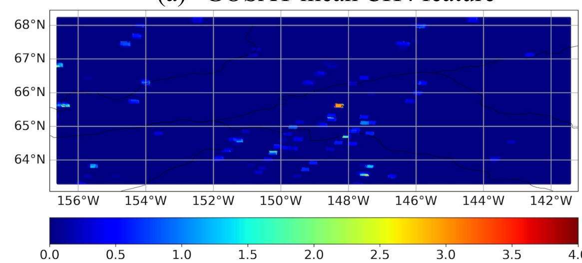

(b) GOSAT variance CH4 feature

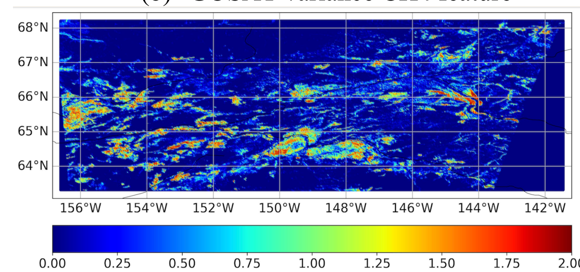

(c) Land-cover feature

Figure 6: Feature data for the Methane Alaska case study. Cloud feature is not shown, refer to Fig. 3 as an example. GOSAT features are the normalized mean/variance of the xCH4 dry air mole fraction measurements at the locations. Land-cover feature is the fraction of grid square which has one of the interesting landcover types: woody wetland, emergent herbaceous wetlands, sedge/herbaceous, grassland/herbaceous.

4. DISCUSSION AND FUTURE WORK

The target prioritization framework can be expected to provide an aid to decision making of target selection by offering a quantitative estimate of the scientific benefits. Multi-day missions could use forecasted information of the days-ahead to further optimize target selection. Further, targets for the subsequent day can be based on what was observed on previous days. Generalizing Targeter parameters to symbolic programming (e.g. Wolfram Alpha language [19]), which can be entered by the users in real-time, would offer more flexibility with reduced complexity. A limitation in our examples is that the *SV* is built by combining disparate data sources in a localized manner. Future work will explore calculating *SV* at a location being dependent on data at other nearby locations which may have some impact.

5. REFERENCES

[1] Saephan, M., Frank, J., Levinson, R., Ravindra, V., Caldwell, D., Duncan, B., Strode, S., Swartz, W., Manies, K., and Turkov, E. (2024). ILEOS: A Novel Intelligent Observing System Enabled by High Altitude Long Endurance Uncrewed Aerial Systems. In AIAA Aviation 2024 Forum.

[2] Chandarana, M., Frank, J., Levinson, R., Turkov, E., Caldwell, D., Ravindra, V., Duncan, B., Strode, S., Swartz, W., and Manies, K. (2023). Intelligent Long Endurance Observing System (ILEOS). Presented at Earth Science Technology Forum. https://esto.nasa.gov/forums/estf2023/Presentations/S9P8_Chandarana_ILEOS_ESTF2023.pdf

[3] Smith, B., Kumar, S., Nguyen, L., Chee, T., Mason, J., Chien, S., ... & Grogan, P. (2022, July). Demonstrating a New Flood Observing Strategy on the NOS Testbed. In IGARSS 2022-2022 IEEE International Geoscience and Remote Sensing Symposium (pp. 5309-5312). IEEE.

[4] Nag, S., Moghaddam, M., Selva, D., Frank, J., Ravindra, V., Levinson, R., ... & Akbar, R. (2021, July). Soil Moisture Monitoring using Autonomous and Distributed Spacecraft (D-SHIELD). In 2021 IEEE International Geoscience and Remote Sensing Symposium IGARSS (pp. 1474-1475). IEEE.

[5] Levinson, R., Niemoeller, S., Nag, S., Ravindra, V. (2022, June). Planning Satellite Swarm Measurements for Earth Science Models: Comparing Constraint Processing and MILP Methods. In Proceedings of the International Conference on Automated Planning and Scheduling (Vol. 32, pp.471-479).

[6] Gorr, B., Ravindra, V., Melebari, A., Aguilar Jaramillo, A., Nag, S., Moghaddam, M., & Selva, D. (2023). Multi-Objective Optimization of an Intelligent Soil-Moisture-Monitoring Satellite Constellation. Journal of Spacecraft and Rockets, 1-13.

[7] Ravindra, V., Roy Singh, S., Moghaddam, M., Nelson, K., Levinson, R., Melebari, A., Kannan, A. (2023). Distributed Spacecraft with Heuristic Intelligence to Enable Logistical Decisions for Global Navigation Satellite System Reflectometry (GNSS-R) of Wildfires. Presented at Earth Science Technology Forum. https://esto.nasa.gov/forums/estf2023/Presentations/S5P3RavindraSinghESTF2023.pdf

[8] Bardaji, J., Bayazid, A., Tapia, J. I., Cho, E., Vuyovich, C., & Grogan, P. T. (2023, July). Constellation Evaluation Tools for a New Snow Observing Strategy. In IGARSS 2023-2023 IEEE International Geoscience and Remote Sensing Symposium (pp. 133-136). IEEE.

[9] Global Modeling and Assimilation Office, NASA Goddard Space Flight Center. (n.d.). GEOS Near Real-Time (NRT) Products. https://gmao.gsfc.nasa.gov/GMAO_products/NRT_products.php

[10] Veefkind, J. P., Aben, I., McMullan, K., Förster, H., de Vries, J., Otter, G., et al. (2012). TROPOMI on the ESA Sentinel-5 Precursor: A GMES mission for global observations of the atmospheric composition for climate, air quality and ozone layer applications. Remote Sensing of Environment, 120(2012), 70–83. https://doi.org/10.1016/j.rse.2011.09.027

[11] Van Geffen, J. H. G. M., Eskes, H. J., Boersma, K. F., Maasakkers, J. D., & Veefkind, J. P. (2019). TROPOMI ATBD of the total and tropospheric NO2 data products. Retrieved from http://www.tropomi.eu/sites/default/files/files/publicS5P-KNMI-L2-0005-RP-ATBD_NO2_ data_products-20190206_v140.pdf

[12] Goldberg, D. L., Anenberg, S. C., Kerr, G. H., Mohegh, A., Lu, Z., & Streets, D. G. (2021). TROPOMI NO2 in the United States: A detailed look at the annual averages, weekly cycles, effects of temperature, and correlation with surface NO2 concentrations. Earth's Future, 9, e2020EF001665. https://doi.org/10.1029/2020EF001665

[13] Jet Propulsion Laboratory, California Institute of Technology. (Nov 2022). Airborne Visible/ Infrared Imaging Spectrometer AVIRIS-Next Generation. https://avirisng.jpl.nasa.gov/ (Accessed January 4, 2024).

[14] Centre for Environmental Data Analysis (CEDA). (n.d.). University of Leicester GOSAT Proxy XCH4 v9.0. https://data.ceda.ac.uk/neodc/gosat/data/ch4/nceov1.0/CH4_GOS_OCPR

[15] National Institute for Environmental Studies. (n.d.). Greenhouse gases observing satellite GOSAT "IBUKI" https://www.gosat.nies.go.jp/en/

[16] Parker, R. J. and Webb, A. and Boesch, H. and Somkuti, P. and Barrio Guillo, R. and Di Noia, A. and Kalaitzi, N. and Anand, J. S., et al. 2020, "A decade of GOSAT Proxy satellite CH4 observations," Earth System Science Data, Vol 12, pp. 3383—3412 https://essd.copernicus.org/articles/12/3383/2020/

[17] Dewitz, J., and U.S. Geological Survey, 2021, National Land Cover Database (NLCD) 2019 Products (ver. 2.0, June 2021): U.S. Geological Survey data release, https://doi.org/10.5066/P9KZCM54

[18] Multi-Resolution Land Characteristics (MRLC) Consortium. (n.d.). NLCD 2016 Land Cover - Alaska. https://www.mrlc.gov/data/nlcd-2016-land-cover-alaska/

[19] Wolfram. (n.d.). Wolfram Language. https://www.wolfram.com/language/ (Accessed April 30, 2024).